Cell

Telomerase Reverse Transcriptase Delays Aging in Cancer-Resistant Mice

Antonia Tomás-Loba,[1,5] Ignacio Flores,[1,5] Pablo J. Fernández-Marcos,[2] María L. Cayuela,[1,6] Antonio Maraver,[2] Agueda Tejera,[1] Consuelo Borrás,[3] Ander Matheu,[2] Peter Klatt,[1,2] Juana M. Flores,[4] José Viña,[3] Manuel Serrano,[2] and Maria A. Blasco[1,*]

[1]Telomeres and Telomerase Group
[2]Tumor Suppression Group
Molecular Oncology Program, Spanish National Cancer Centre (CNIO), Madrid 28029, Spain
[3]Department of Physiology, University of Valencia, Valencia 46010, Spain
[4]Department of Animal Surgery and Medicine, Complutense University of Madrid, Madrid 28040, Spain
[5]These authors contributed equally to this work
[6]Present address: Hospital Virgen de la Arrixaca, Murcia 30120, Spain
*Correspondence: mblasco@cnio.es
DOI 10.1016/j.cell.2008.09.034

SUMMARY

Telomerase confers limitless proliferative potential to most human cells through its ability to elongate telomeres, the natural ends of chromosomes, which otherwise would undergo progressive attrition and eventually compromise cell viability. However, the role of telomerase in organismal aging has remained unaddressed, in part because of the cancer-promoting activity of telomerase. To circumvent this problem, we have constitutively expressed telomerase reverse transcriptase (TERT), one of the components of telomerase, in mice engineered to be cancer resistant by means of enhanced expression of the tumor suppressors p53, p16, and p19ARF. In this context, TERT overexpression improves the fitness of epithelial barriers, particularly the skin and the intestine, and produces a systemic delay in aging accompanied by extension of the median life span. These results demonstrate that constitutive expression of *Tert* provides antiaging activity in the context of a mammalian organism.

INTRODUCTION

Aging is a multifactorial process that has been adjusted by nature to a wide spectrum of life spans, even in closely related species, thus suggesting that aging is a flexible trait susceptible to the influence of a number of molecular pathways (Brown-Borg et al., 1996; Haigis and Guarente, 2006; Kenyon, 2005). One such process is the progressive attrition of telomeres that occurs in association with organismal aging in humans (Harley et al., 1990) and in other mammals, such as mice (Flores et al., 2008). Telomeres are specialized structures at the ends of chromosomes that have a role in protecting the chromosome ends from DNA repair and degrading activities (Blackburn, 2001; de Lange, 2005). Mammalian telomeres consist of TTAGGG repeats bound by a multiprotein complex known as shelterin (de Lange, 2005). A minimum length of TTAGGG repeats and the integrity of the shelterin complex are necessary for telomere protection (Blackburn, 2001; de Lange, 2005). Telomerase is a cellular reverse transcriptase (TERT, telomerase reverse transcriptase) capable of compensating telomere attrition through de novo addition of TTAGGG repeats onto the chromosome ends by using an associated RNA component as template (*Terc*, telomerase RNA component) (Greider and Blackburn, 1985). Telomerase is expressed in most adult stem cell compartments; however, this is not sufficient to maintain telomere length, as evidenced by the fact that telomere shortening occurs with age in most human and mouse tissues (Harley et al., 1990; Blasco, 2007; Flores et al., 2008). Furthermore, some diseases characterized by premature loss of tissue renewal and premature death, such as dyskeratosis congenita, anemia, and idiopathic pulmonary fibrosis, are linked to germline mutations in *Tert* and *Terc* genes, which result in decreased telomerase activity and accelerated telomere shortening (Mitchell et al., 1999; Vulliamy et al., 2001; Yamaguchi et al., 2005; Tsakiri et al., 2007; Armanios et al., 2007). A role for telomerase in tissue renewal and organismal life span is also supported by telomerase-deficient ($Terc^{-/-}$) mice (Blasco et al., 1997). Longevity is progressively shortened upon successive intercrossing of telomerase-deficient mice (Blasco, 2005), an effect already noticeable at the first generation of *Terc* null mice where both the median and maximum life span are reduced (Garcia-Cao et al., 2006). Finally, telomerase overexpression is sufficient to extend the life span of most human cells in culture (Bodnar et al., 1998). Together, the evidence strongly suggests that telomerase activity and telomere length are rate limiting for mammalian life span and supports a model in which short telomeres actively contribute to aging by limiting tissue renewal. An important prediction of this model is that slowing the rate of telomere shortening should delay aging. However, to address experimentally this prediction, it is necessary to take into account the role of telomere biology in cancer.

Telomere shortening is an important barrier for the uncontrolled proliferation of tumor cells (Feldser and Greider, 2007; Blasco, 2005). In this context, it is not surprising that constitutive telomerase expression in several independent *Tert*-transgenic mouse

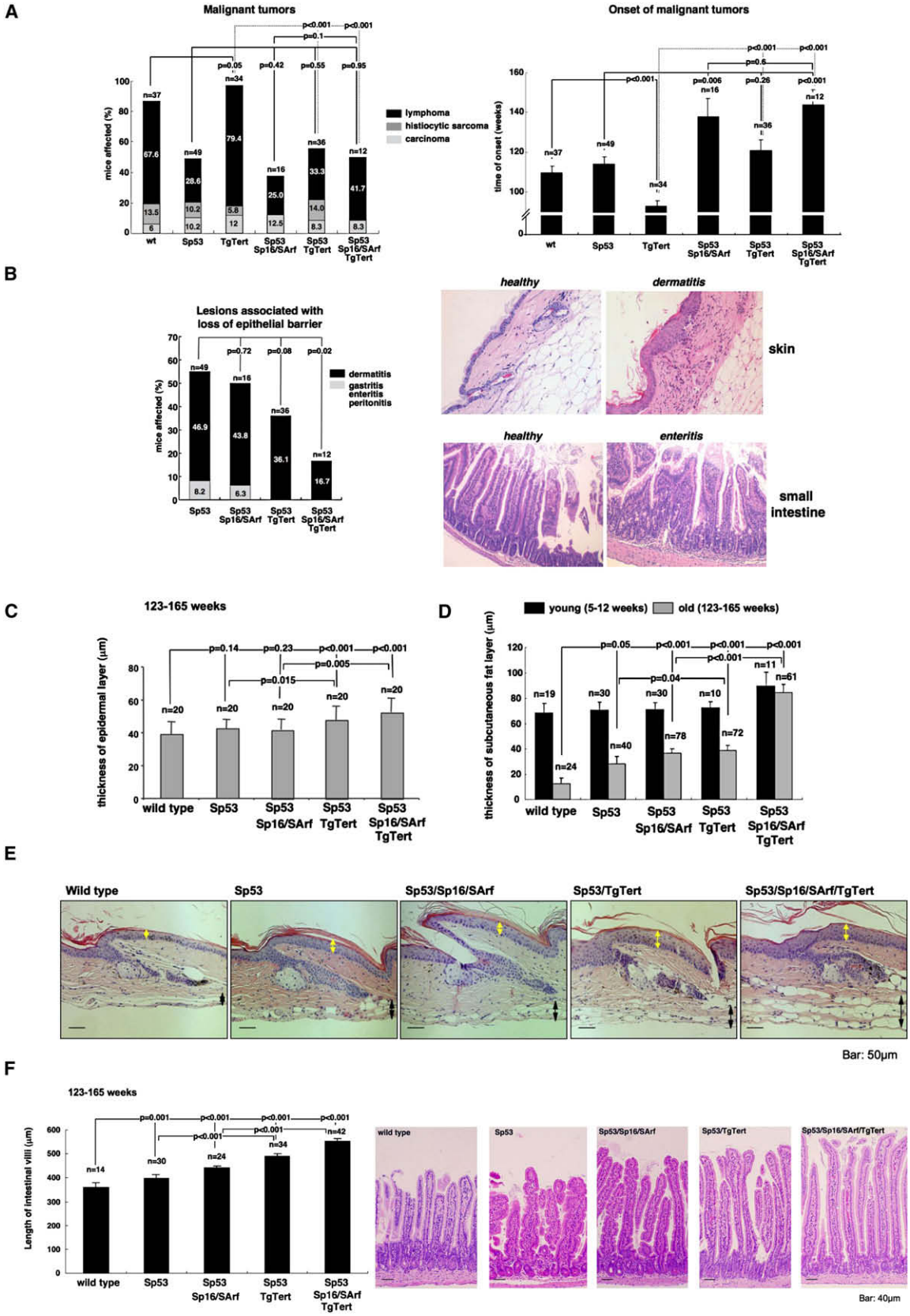
A
Malignant tumors
mice effected (%)
lymphoma
histiocytic sarcoma
carcinoma
wt
Sp53
TgTert
Sp53 Sp16/SArf
Sp53 TgTert
Sp53 Sp16/SArf TgTert
Onset of malignant tumors
time of onset (weeks)
B
Lesions associated with loss of epithelial barrier
mice affected (%)
dermatitis
gastritis
enteritis
peritonitis
healthy
dermatitis
skin
healthy
enteritis
small intestine
C
123-165 weeks
thickness of epidermal layer (µm)
wild type
Sp53
Sp53 Sp16/SArf
Sp53 TgTert
Sp53 Sp16/SArf TgTert
D
young (5-12 weeks)
old (123-165 weeks)
thickness of subcutaneous fat layer (µm)
E
Wild type
Sp53
Sp53/Sp16/SArf
Sp53/TgTert
Sp53/Sp16/SArf/TgTert
Bar: 50µm
F
123-165 weeks
Length of intestinal villi (µm)
Bar: 40µm

models resulted in increased incidence of spontaneous tumors (González-Suárez et al., 2001; González-Suárez et al., 2002; Artandi et al., 2002; Canela et al., 2004). Therefore, in normal laboratory mice, the advantageous impact of telomerase on cancer cells obscures the potentially beneficial effects of telomerase in the context of normal cells and tissues; for this reason, we have resorted to cancer-resistant mice previously generated by us (Garcia-Cao et al., 2002; Matheu et al., 2004; 2007). In particular, by transgenesis using large, nonmanipulated, genomic segments, we have generated mice carrying a single transgenic copy of *p53* or a single transgenic copy of the locus encoding *Arf* and *p16* (Garcia-Cao et al., 2002; Matheu et al., 2004). These three tumor suppressors are involved in protection against a large variety of cancers (Collado et al., 2007). The above-mentioned transgenic mice, which we call super-*p53* (*Sp53*) or super-*p16*/*Arf* (*Sp16*/*SArf*), possess three gene doses of each of the indicated tumor suppressors instead of the normal diploid gene dose; this increase in tumor suppression activity is sufficient to significantly increase cancer resistance (Garcia-Cao et al., 2002; Matheu et al., 2004). Of relevance, single transgenic *Sp53* or *Sp16*/*SArf* mice have a normal aging and life span (Garcia-Cao et al., 2002; Matheu et al., 2004), but the combination of both transgenes in doubly transgenic *Sp53*/*Sp16*/*SArf* mice results in delayed aging, probably because of the ability of these tumor suppressors to eliminate cellular damage and damaged cells (Matheu et al., 2007).

Here, we address the role of telomerase in mouse fitness and aging by generating *Tert*-transgenic mice in a tumor-resistant genetic background, in an effort to dissociate the effects of telomerase on cancer and aging. In this context, we demonstrate that *Tert* overexpression has antiaging activity.

RESULTS

Generation of Cancer-Resistant Mice with Increased TERT Levels

Mice that constitutively express the telomerase *Tert* gene in the stem and proliferative compartments of a wide range of epithelial tissues (*K5-Tert* mice, González-Suárez et al., 2001, 2002; referred hereafter as *TgTert*), were crossed with cancer-resistant *Sp53* and *Sp16*/*SArf* mice (Garcia-Cao et al., 2002; Matheu et al., 2004; 2007). The resulting *Tert*-transgenic mice with increased tumor resistance were named *Sp53*/*Sp16*/*SArf*/*TgTert* mice. *TgTert* tissues show $\leq$10-fold increase in telomerase activity compared to wild-type tissues (González-Suárez et al., 2001, 2002), which is within the range of telomerase activation upon various stimuli, such as T cell activation (Buchkovich and Greider, 1996) or *myc* expression (Flores et al., 2006). *TgTert*-associated phenotypes include increased wound healing, improved epidermal stem cell mobilization/proliferation, and increased tumorigenesis (González-Suárez et al., 2001, 2002; Flores et al., 2005; 2006). These effects of *Tert* overexpression are noticeable already at young ages and require the telomerase *Terc* component (Flores et al., 2005, 2006; Cayuela et al., 2005), thus suggesting that they are the consequence of increased telomerase activity and longer telomeres in these mice. Nevertheless, it is relevant to note that other authors have suggested additional roles of *Tert* overexpression on stem cell proliferation, which are independent of telomerase activity (Sarin et al., 2005) and could also have a positive impact on aging and longevity.

We used a single set of parental mice (*TgTert* × *Sp53*/*Sp16*/*SArf*) to obtain two pairs of cancer-resistant strains—namely, *Sp53* and *Sp53*/*TgTert* strains, and *Sp53*/*Sp16*/*SArf* and *Sp53*/*Sp16*/*SArf*/*TgTert* strains (see Experimental Procedures). We first analyzed whether the tumorigenic effects of the *Tert* transgene (Figure 1A) had been canceled in the *Sp53* and *Sp53*/*Sp16*/*SArf* backgrounds. Importantly, both the incidence and time of onset of malignant tumors (lymphomas, sarcomas, and carcinomas) did not differ significantly between *Sp53* and *Sp53*/*TgTert* cohorts, or between *Sp53*/*Sp16*/*SArf* and *Sp53*/*Sp16*/*SArf*/*TgTert* mice (Figure 1A), thus indicating that the tumorigenic effects of *TgTert* have been effectively canceled in these backgrounds.

TERT Expression Decreases Aging-Associated Pathologies

Degenerative inflammatory pathologies of the skin (dermatitis) and of the gastrointestinal (GI) tract (gastritis, enteritis, and peritonitis) are common in aged mice and are often associated with increased susceptibility to pathogens or external antigens. Analysis of these lesions in aged mice indicated that *TgTert*-expressing mice have a decreased incidence of degenerative inflammatory pathologies in both cancer-resistant contexts (*Sp53* background and *Sp53*/*Sp16*/*SArf* background; $p = 0.02$ and $p = 0.08$, respectively; Figure 1B). Although a direct effect of *Tert* expression on the long-term function of the immune system cannot be dismissed, these results also suggest that telomerase may contribute to a more robust maintenance of the skin and GI epithelia. To further support this, we analyzed morphological criteria of aging in these tissues. The thinning of the subcutaneous adipose layer is a known aging-associated morphological feature, which, in turn, is associated with increased risk of skin injuries and infections. Aged *Sp53*/*TgTert* and *Sp53*/*Sp16*/*SArf*/*TgTert* mice showed a better preservation of both the thickness of the epidermis and of the subcutaneous fat layer compared to their corresponding *Sp53* and *Sp53*/*Sp16*/*SArf* controls

Figure 1. Delayed Cancer and Aging in *Sp53*/*Sp16*/*SArf*/*TgTert* Mice

(A) Mice showing malignant tumors at the time of death (i.e., moribund mice sacrificed hours before death). n, number of mice. Data are given as mean ± standard error of the mean (SEM).

(B) Percentage of mice showing the indicated degenerative lesions at the time of death. Representative images are also shown.

(C) Thickness of the outer skin layer (epidermis) in mice of the indicated genotypes. n, number of independent measurements from at least three mice per genotype. Data are given as mean ± SEM.

(D) Thickness of the subcutaneous fat layer. Note thinning of the subcutaneous fat layer with increasing mouse age. In contrast, *Sp53Sp53*/*Sp16*/*SArf*/*TgTert* mice preserve a normal subcutaneous fat layer at old ages. Data are given as mean ± SEM.

(E) Representative images of skin sections. Yellow arrows, interfollicular epidermis. Black arrows, subcutaneous sebaceous layer.

(F) Length of the intestinal villi. n, number of independent measurements from at least three mice per genotype. Data are given as mean ± SEM. Representative small intestine images are shown in the bottom panel.

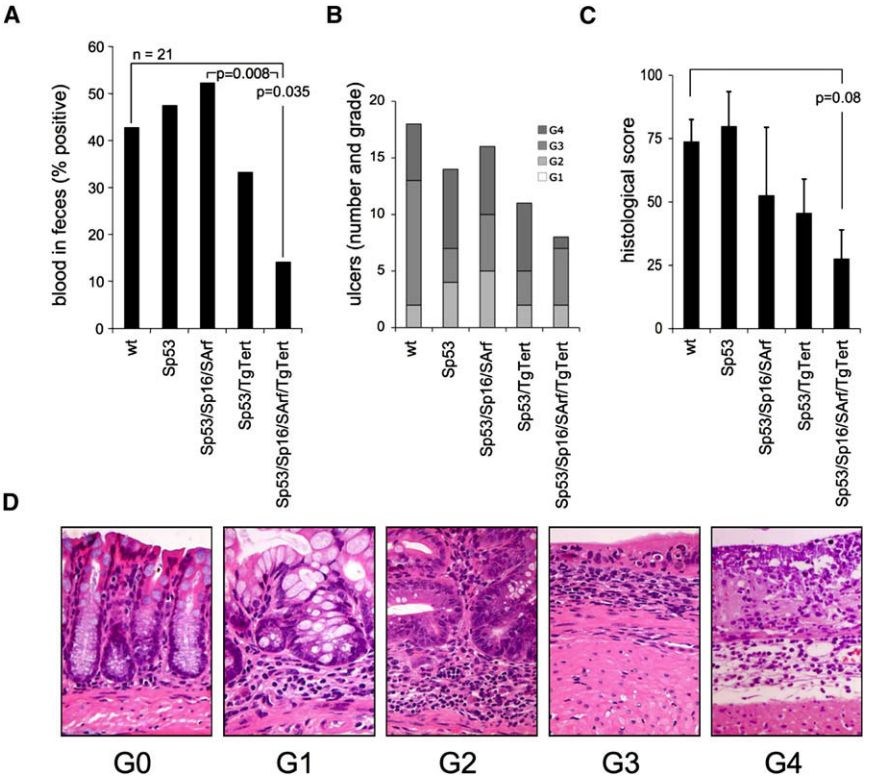

Figure 2. Improved GI Tract Epithelial Barrier Function in *Sp53/Sp16/SArf/TgTert* Mice

(A) Intestinal sensitivity to dextrane (DSS). Percentage of blood-positive feces in 21–51-week-old mice at days 3, 5, and 7 after treatment with DSS 2%. The total number of fecal pellets (n = 21) analyzed from a total of 5 mice per genotype is indicated. Data are given as mean ± SEM.

(B) Total number of ulcers at day 7 posttreatment. Ulcers are classified according to their grade (Experimental Procedures and panel D).

(C) Histological score of the ulcers obtained by multiplying the score and the size of the ulcers (Experimental Procedures). Data are given as mean ± SEM.

(D) Representative examples of ulcer grades.

($p < 0.05$ for all comparisons; Figures 1C and 1E). Similarly, we also detected a better preservation of the GI tract epithelia (length of the villi) in the *TgTert*-expressing genotypes at old age compared with their non-*TgTert* controls ($p < 0.001$ for both comparisons; Figure 1F). To address whether these mice had an improved epithelial barrier function in the GI tract, we treated mice with dextran sodium sulfate (DSS), a well-established inducer of intestinal ulcers (Rakoff-Nahoum et al., 2004). Interestingly, *Sp53/Sp16/SArf/TgTert* mice were more resistant to DSS than were wild-type and *Sp53/Sp16/SArf* controls, as indicated by decreased intestinal bleeding and a lower number and grade of ulcers following DSS treatment (Figures 2A–2D) (Experimental Procedures). A similar protective effect of *TgTert* was observed when *Sp53/TgTert* mice were compared to *Sp53* mice (Figures 2A–2D). Finally, the onset of a large variety of age-related pathologies, mostly atrophies and inflammatory processes, was also significantly delayed in *Sp53/Sp16/SArf/TgTert* mice, compared with the *Sp53* and *Sp53/Sp16/SArf* controls ($p < 0.05$ in both cases; see Figure S1 and the Supplemental Experimental Procedures available online). Altogether, these results indicate that, in two independent cancer-resistant backgrounds (*Sp53* and *Sp53/Sp16/SArf* mice), *TgTert* expression provides improved fitness to epithelial barriers and protection against aging-associated degenerative and inflammatory processes.

Sp53/Sp16/SArf/TgTert Mice Exhibit Improved Neuromuscular Coordination and Glucose Tolerance Compared to Age-Matched Controls

Antiaging manipulations targeted at a single tissue can result in systemic antiaging effects, as illustrated by mice lacking the insulin receptor exclusively in the adipose tissue and showing an extended longevity (Blüher et al., 2003), or by systemic antiaging effects mediated by soluble factors in the blood (Conboy et al., 2005). Along these lines, we wondered whether targeted *Tert* expression to epithelial tissues, as performed here, in cancer-resistant mice also had systemic antiaging effects. To this end, we analyzed various additional well-established biomarkers of aging, such as the progressive loss of neuromuscular coordination (Ingram and Reynolds, 1986), which can be measured with the so-called tightrope test (see Experimental Procedures). Interestingly, tightrope test performance was significantly improved in *Sp53/Sp16/SArf/TgTert* mice at $\geq$1 years of age, compared with age-matched wild-type and *Sp53/Sp16/SArf* controls ($p < 0.05$ for both comparisons; Figures 3A and 3B), and the contribution of *TgTert* was also significant in the *Sp53/TgTert* mouse cohort, compared with both wild-type and *Sp53* controls ($p \leq 0.04$; Figures 3A and 3B).

Metabolic disorders, such as glucose intolerance, have been also associated with aging (Goren et al., 2004). Interestingly, both *Sp53/TgTert* and *Sp53/Sp16/SArf/TgTert* mice showed a significantly improved glucose tolerance, compared with the other genotypes, as indicated by a better glucose uptake following glucose injection ($p < 0.05$ in both cases, Figure 3C; see Figure S2 for complete glucose curves). Finally, using metabolic cages, we observed no gross differences in food or water intake, or in feces and urine output, between the different genotypes (see Experimental Procedures) (Figure S3). In addition, body weights were similar in both males and females at young and old ages in the different mouse cohorts (Figure S4), in agreement with the fact that these mice were not calorie restricted and had ad libitum access to food.

Higher Serum IGF1 Levels and Decreased γ-H2AX Foci in *Sp53/Sp16/SArf/TgTert* Mice

Although lifelong exposure to low IGF1 extends life span (Brown-Borg et al., 1996; Murphy et al., 2003), it is also known that IGF1

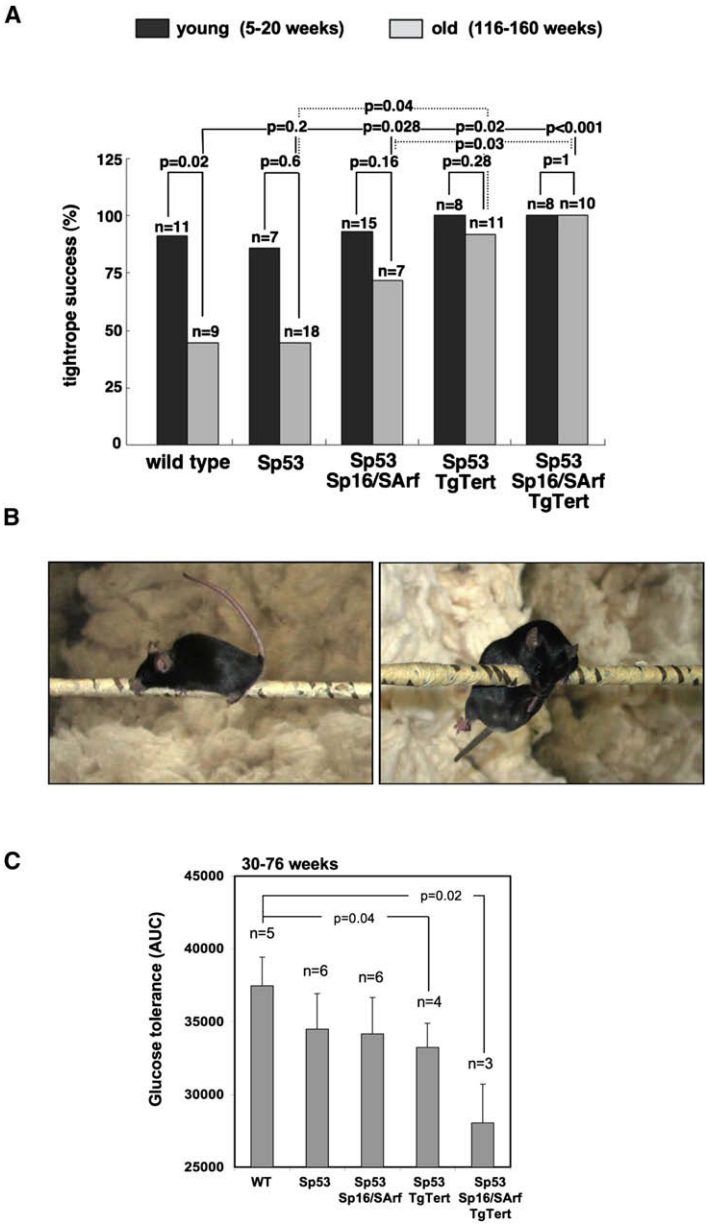

Figure 3. Decreased Biomarkers of Aging in *Sp53/Sp16/SArf/TgTert* Mice

(A) Neuromuscular coordination was quantified as the percentage of mice that successfully passed the tightrope test. n, number of mice.

(B) Representative images show the design of the test.

(C) Glucose tolerance measured as the area under the curve (AUC) representing glucose concentration in blood at different times post-glucose i.p. injection (Figure S2 for glucose curves). n = number of mice (30–76 weeks old). Data are given as mean ± SEM.

levels decrease with aging (Hammerman, 1987). In addition, some mouse models of premature aging present an accelerated decrease in IGF1 (Niedernhofer et al., 2006), suggesting that decreased IGF1 signaling in aged mice could be secondary to organismal decay. Interestingly, old *Sp53/Sp16/SArf/TgTert* mice showed significantly higher serum IGF1 levels compared with age-matched wild-type and *Sp53/Sp16/SArf* controls ($p = 0.02$ in both cases; Figure 4); similar differences were observed in young mice from both *Sp53/TgTert* and *Sp53/Sp16/SArf/TgTert* genotypes (Figure 4A). These observations suggest that the delayed aging of these mice is not the consequence of decreased serum IGF1 levels. High serum IGF1 levels in *Sp53/TgTert* and *Sp53/Sp16/SArf/TgTert* mice may explain their improved glucose uptake and their improved neuromuscular coordination, because IGF1 has been described to act as a insulin mimetic (Yuen and Dunger, 2007) and to have beneficial effects on neuromuscular fitness (Delbono, 2003), respectively.

We previously described that *Sp53/Sp16/SArf* mice show decreased levels of oxidized proteins and oxidized lipids both at young and old ages as the result of a higher expression of the antioxidant *p53*-target genes *Sesn1* and *Sesn2* (Matheu et al., 2007), in agreement with the recently proposed antioxidant role for p53 (Sablina et al., 2005). However, analysis of protein oxidation in liver (Figure S5 and Supplemental Experimental Procedures), and expression of antioxidant p53 targets (Figure S6), indicated that they were not specifically affected by *TgTert* and therefore could not explain its longevity effects. Similarly, activation of the *p16/Arf* locus, which is one of the most dramatic molecular changes associated with organismal aging (Matheu et al., 2007; Krishnamurthy et al., 2004; Zindy et al., 1997), was not significantly affected by telomerase (Figure S7), thus indicating that the delayed aging of *Sp53/Sp16/SArf/TgTert* mice is not due to a lower activation of the *p16/Arf* locus in these mice.

A recently described molecular marker of aging is the accumulation of phosphorylated histone H2AX (γ-H2AX) foci in aged tissues, which is thought to reflect the accumulation of DNA double strand breaks, including those derived from critically short/dysfunctional telomeres (Sedelnikova et al., 2004; Herbig et al., 2006; d'Adda di Fagagna et al., 2003). As shown in Figures 4C–4F, γ-H2AX-positive cells were increased both in the skin and the esophagus of old wild-type and *Sp53* mice compared with younger counterparts, but this aging-dependent increase in γ-H2AX foci was significantly attenuated by the presence of *TgTert* in the *Sp53/TgTert* and *Sp53/Sp16/SArf/TgTert* mouse cohorts compared with both wild-type mice and to their corresponding *Sp53* and *Sp53/Sp16/SArf* controls (Figures 4C–4F). Of note, old *Sp53/Sp16/SArf* mice also showed significantly lower frequencies of γH2AX-positive cells, in agreement with the reported synergic effect of p19ARF and p53 in decreasing aging-associated DNA damage (Matheu et al., 2007). Importantly, the presence of *TgTert* completely eliminated the telomeric γ-H2AX signals in the skin of *Sp53/TgTert* and *Sp53/Sp16/SArf/TgTert* mice, as indicated by a lack of colocalization of γ-H2AX foci with the TRF1 telomeric protein (Figures 4H and 4I). These results suggest that *TgTert* expression is particularly efficient at eliminating DNA damage associated with dysfunctional telomeres.

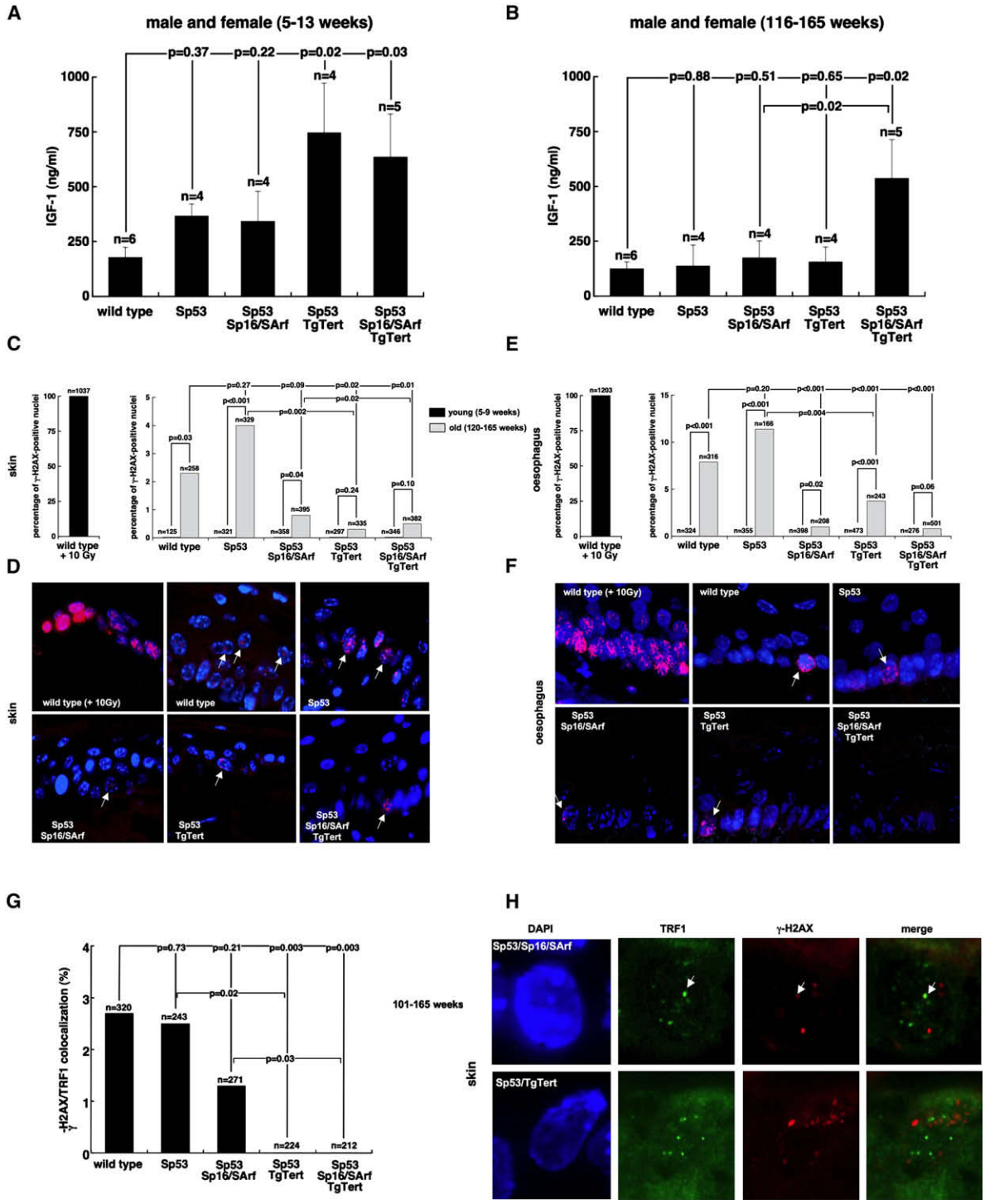

Figure 4. Decreased Molecular Markers of Aging in *Sp53/Sp16/SArf/TgTert* Mice

(A and B) IGF1 serum levels in renal and retro-orbital cavity blood from young (A) and aged (B) mice of the indicated genotypes. Data are mean ± SEM; n, number of mice. Skin (C and D) and esophagus (E and F) sections from young and aged mice were analyzed for the percentage (C and D) of γ-H2AX positive nuclei by confocal microscopy. γ-irradiated wild-type skin was included as positive control. Representative images (D and F) of γ-H2AX positive cells (indicated by white arrows) are shown. The χ^2 test was used for statistical comparisons. A cell was considered positive for γ-H2AX when it showed more than 2 signals. n, number of cells from a total of three mice per genotype.

(G and H) Colocalization of γ-H2AX and TRF1 foci (TIF) by confocal microscopy. Representative images (H) are shown for *Sp53/Sp16/SArf* (1 colocalization event) and *Sp53/TgTert* (no colocalization events) genotypes. The Fisher's exact test was used for statistical comparisons. A cell was considered positive when one or more γ-H2AX foci colocalized with TRF1 signals.

All together, the analysis of a variety of aging-associated pathologies (degenerative and inflammatory lesions), biomarkers of aging (including subcutaneous fat layer, epithelial barrier function, neuromuscular coordination, and glucose tolerance), and molecular markers of aging (IGF1, DNA damage, telomere-associated DNA damage) strongly indicate that the *TgTert* allele improves organismal fitness and delays aging.

Increased Median Life Span in *Sp53/Sp16/SArf/TgTert* Mice

Given the above-described antiaging activity of telomerase, we next addressed whether the *TgTert* allele had a detectable effect on the life span of cancer-resistant *Sp53* and *Sp53/Sp16/SArf* mice. To this end, we obtained survival curves covering the entire life span of *Sp53/TgTert* and *Sp53/Sp16/SArf/TgTert* mice, compared with *Sp53* and *Sp53/Sp16/SArf* controls; all these mice have the same genetic background composition of 75%:25% C57BL6/DBA (see Experimental Procedures). *Sp53* mice were used as a reference for normal longevity in our mouse cohorts because they have been previously shown to have the same longevity as wild-type mice in two independent studies (Garcia-Cao et al., 2002; Matheu et al., 2007). Of note, we did not observe a significant difference in the survival of *Sp53* mice or *Sp53/Sp16/SArf* control mice, whether in a pure 100% C57BL6 background or in a mixed 75%:25% C57BL6/DBA background, indicating that the 25% DBA contribution does not affect longevity in our mouse cohorts (Figure S8). Analysis of the survival curves indicated a significant extension of median life span of 9% and 26% by *TgTert* expression in the context of cancer-resistant *Sp53* and *Sp53/Sp16/SArf* mice, respectively ($p = 0.05$; Figure 5A). To further dissociate the effects of *TgTert* expression on cancer and aging, we considered separately the life span of cancer-free mice (i.e., those mice that died without malignant tumors; Figure S9). In this subgroup of mice, whose life spans are determined by aging and not by cancer, the impact of *TgTert* expression was even more evident, resulting in a median life span extension of 18% and 38% in *Sp53/TgTert* and *Sp53/Sp16/SArf/TgTert* mice, respectively, compared with the *Sp53* and *Sp53/Sp16/SArf* controls (Figure S9). Furthermore, combined *TgTert* and *Sp53/Sp16/SArf* transgenes resulted in a 40.2% extension of the median life span when compared to single *Sp53* mice (our reference for normal longevity), which was further increased to 50% when considering cancer-free mice (Figure S9). To estimate whether *TgTert* expression had an effect on maximum longevity, we studied the group of longest-lived mice of each genotype. First, the percentage of mice that reached the extremely old age of 3 years is significantly larger for *Sp53/Sp16/SArf/TgTert* mice than for their *Sp53/Sp16/SArf* controls (42% versus 8%; Figure 5B), and this extreme old survival is further increased when considering cancer-free mice (up to 50%; Figure S9). Second, the mean age of the upper longevity quartile is significantly higher in *Sp53/Sp16/SArf/TgTert* mice than in their *Sp53/Sp16/SArf* controls (163 weeks versus 146 weeks; $p < 0.01$; Figure 5C). These observations indicate that *TgTert* expression changes the longevity curve of mice, significantly extending the median life span and significantly increasing the percentage of mice that reach extremely old ages. In addition to its well-established telomere-maintenance activity, there is evidence for nontelomeric activities of TERT that can be exerted in the absence of its catalytic activity (Sarin et al., 2005). We wondered whether the observed effects of telomerase on longevity required its telomere-maintenance activity; for this, we examined the longevity curve of *TgTert* mice lacking the RNA component of telomerase (*Terc*), which is essential for telomerase catalytic activity. We observed that *TgTert* does not have an effect on the longevity curve of *Terc*-deficient mice across different generations up to the fourth generation (G2–G4) (Figure 5D). Similarly, *TgTert* does not have a significant effect on the incidence of cancer and aging pathologies in G1–G4 *Terc*-deficient mice (Figures 5E–5G), in marked contrast to *TgTert* mice in a wild-type *Terc* background (see Figure 1A). These results indicate that the antiaging activity of TERT requires telomerase catalytic activity, strongly implicating telomere maintenance as the main mechanism underlying the longevity effect of *TgTert* expression.

TERT Expression Delays Telomere Loss with Age

One of the best known molecular mechanisms of aging is the progressive attrition of telomeres with age both in humans and mice (Harley et al., 1990; Flores et al., 2008). We have recently shown that mouse telomeres suffer significant shortening at old ages (>2 years old), in both the stem cell and differentiated compartments of a wide range of tissues, which is concomitant with decreased telomerase activity (Flores et al., 2008). These results suggest that failure to proficiently maintain telomeres at old ages may significantly contribute to mouse aging (Flores et al., 2008). Here, we address whether the beneficial effects of the *TgTert* allele on mouse fitness and aging, even at young ages, could be related to the biology of telomeres. Telomerase activity was significantly increased in skin keratinocytes derived from old *Sp53/TgTert* and *Sp53*/Sp16/SArf/*TgTert* mice compared with age-matched wild-type mice and with their respective *Sp53* and *Sp53*/Sp16/SArf controls ($p < 0.05$ for all comparisons, Figures 6A and 6B). Coincidental with higher telomerase activity in *TgTert* mice, we observed significantly longer telomeres and a lower percentage of short telomeres in both the skin and keratinocyte metaphases derived newborn mice (Figures S10A–S10E), suggesting that *TgTert* expression decreases telomere erosion associated with normal skin homeostasis already at very young ages, in agreement with *TgTert* promoter expression (keratin 5) from day 11.5 of embryonic development (Ramírez et al., 1994). Next, we analyzed telomere length in both the stem cell (hair bulge) and differentiated (interfollicular epidermis) compartments of the skin using a high-resolution telomere Q-FISH technique based on confocal microscopy, which allows generating telomere length maps within tissues (“telomapping”) (Flores et al., 2008). Telomapping confirmed telomere shortening with age in wild-type mice, as well as the presence of longer telomeres in the stem cell compartment compared with the more differentiated compartments (Figures 6C–6E) (Flores et al., 2008). Importantly, telomapping showed that old *Sp53*S/Sp16/SArf/*TgTert* mice had the highest average telomere length compared with the other genotypes both in the stem cell (hair bulge) and differentiated compartments (interfollicular epidermis) of the skin (Figures 6C–6E and S11). Concomitant with this, old *Sp53*/Sp16/SArf/*TgTert* mice had the lowest percentage of cells with

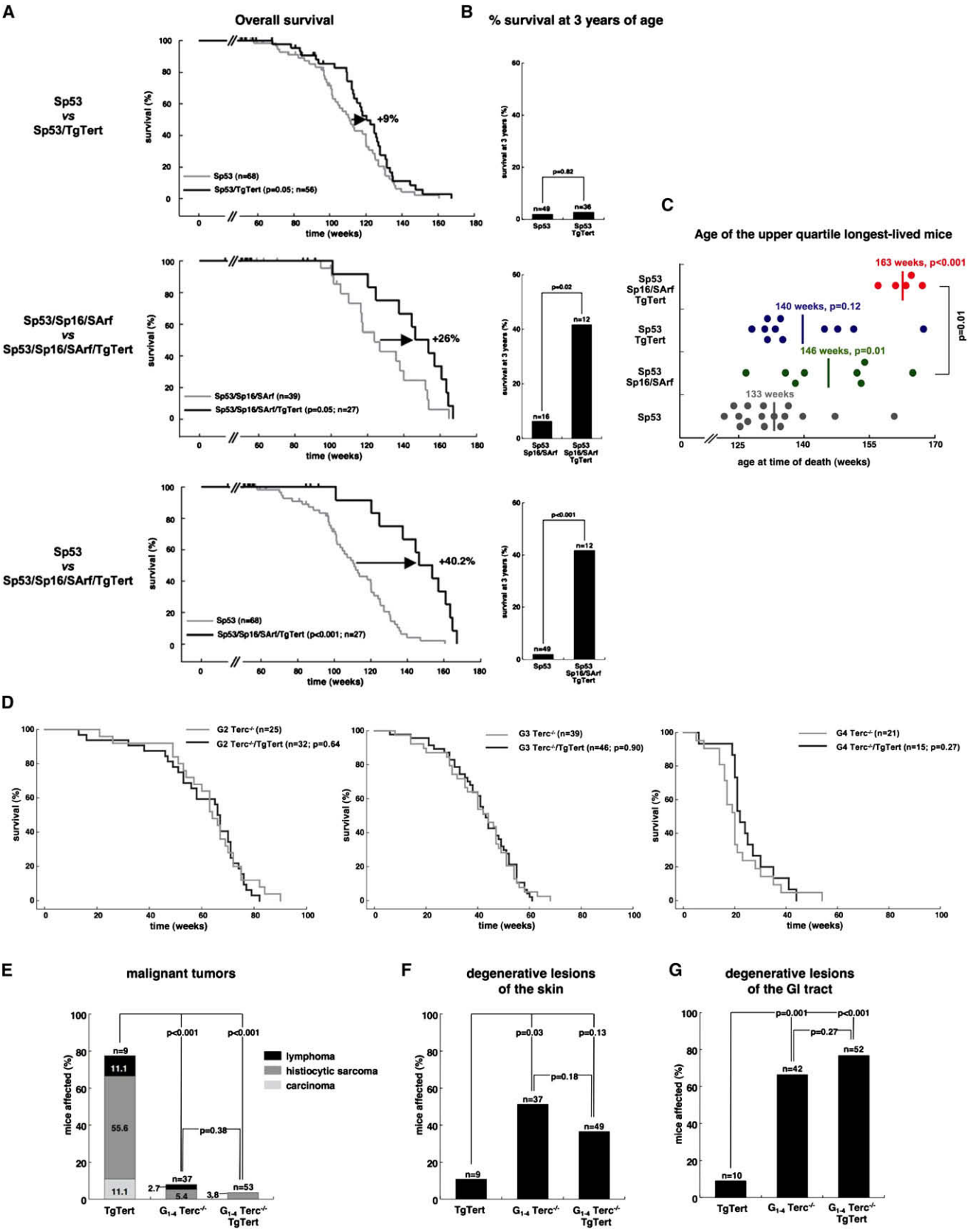
A
Overall survival
Sp53
vs
Sp53/TgTert
survival (%)
time (weeks)
+9%
Sp53 (n=68)
Sp53/TgTert (p=0.05; n=56)
B
% survival at 3 years of age
survival at 3 years (%)
p=0.82
n=49
n=36
Sp53
Sp53 TgTert
Sp53/Sp16/SArf
vs
Sp53/Sp16/SArf/TgTert
+26%
Sp53/Sp16/SArf (n=39)
Sp53/Sp16/SArf/TgTert (p=0.05; n=27)
p=0.02
n=16
n=12
Sp53 Sp16/SArf
Sp53 Sp16/SArf TgTert
Sp53
vs
Sp53/Sp16/SArf/TgTert
+40.2%
Sp53 (n=68)
Sp53/Sp16/SArf/TgTert (p<0.001; n=27)
p<0.001
n=49
n=12
C
Age of the upper quartile longest-lived mice
163 weeks, p<0.001
140 weeks, p=0.12
146 weeks, p=0.01
133 weeks
p=0.01
Sp53 Sp16/SArf TgTert
Sp53 TgTert
Sp53 Sp16/SArf
Sp53
age at time of death (weeks)
D
G2 Terc-/- (n=25)
G2 Terc-/-/TgTert (n=32; p=0.64
G3 Terc-/- (n=39)
G3 Terc-/-/TgTert (n=46; p=0.90)
G4 Terc-/- (n=21)
G4 Terc-/-/TgTert (n=15; p=0.27)
survival (%)
time (weeks)
E
malignant tumors
mice affected (%)
p<0.001
p<0.001
p=0.38
n=9
11.1
55.6
11.1
n=37
2.7
5.4
3.8
n=53
lymphoma
histiocytic sarcoma
carcinoma
TgTert
G1-4 Terc-/-
G1-4 Terc-/- TgTert
F
degenerative lesions of the skin
p=0.03
p=0.13
p=0.18
n=9
n=37
n=49
G
degenerative lesions of the GI tract
p=0.001
p<0.001
p=0.27
n=10
n=42
n=52

very short telomeres (<10,000 arbitrary units of fluorescence; Figures 6C and 6D), suggesting a decreased rate of telomere shortening. These results were confirmed using conventional quantitative telomere FISH (Q-FISH) (Muñoz et al., 2005) on both skin and esophagus sections (Figure S12), which, in turn, allows for the determination of the percentage of very short telomeres within each nucleus. All together, these findings indicate that *TgTert*-expressing mice have a better preservation of telomeres in epithelial tissues both at young and old ages compared with their respective controls. Interestingly, we noticed that the *Sp53* and *Sp16/SArf* transgenes also had a positive effect on the preservation of telomeres, an effect that could be secondary to a general reduction in proliferation and a better elimination of cells with critically short telomeres.

Increased Clonogenic Activity of *Sp53/Sp16/SArf/TgTert* Epidermal Stem Cells

Telomerase has been reported to improve the regenerative potential of the epidermal stem cells (ESCs), an effect that is probably due to a more robust and resilient maintenance of telomeres but that could also involve non-telomere-dependent mechanisms (Flores et al., 2005; Sarin et al., 2005). To directly address a possible contribution of stem cells to the increased fitness and delayed aging activity of TERT, we performed skin clonogenic assays in both young and old mice expressing or not expressing the *TgTert* allele (Figures 7A and 7B) (see Experimental Procedures). Colonies in this assay have been proposed to derive from individual epidermal stem cells, therefore involving multiple rounds of cell division (Barrandon and Green, 1987; Flores et al., 2005). In agreement with increased telomerase activity and longer telomeres, the *TgTert* genotypes showed increased skin clonogenic potential at both young and old ages, and in both an *Sp53* background and an *Sp53/Sp16/SArf* background (Figures 7A and 7B). Of notice, *TgTert* expression was able to overcome the negative impact of increased p53/p16/p19ARF on ESC clonogenic activity (Figure 7A) (Molofsky et al., 2006). In summary, our results indicate that *Tert* expression preserves the aging-associated loss of telomeres and improves epithelial stem cell function, and both effects could explain its beneficial effects on physiology and aging.

DISCUSSION

The results shown here demonstrate that *Tert* expression can significantly delay aging in mice, although this requires counteracting the protumorigenic effects of telomerase by increasing tumor suppression. The beneficial effects of telomerase are particularly notable in epithelial tissues, which show an improved fitness and a more efficient epithelial barrier function at old ages, resulting in decreased aging-associated inflammatory processes. This is accompanied by an increased longevity of *Tert*-transgenic mice, which present a different longevity curve characterized by a significant increase in median survival and an increase in the percentage of mice reaching extremely old ages.

Analysis of a number of antiaging mechanisms suggests that telomerase exerts its antiaging activity mainly by slowing telomere attrition and by preserving the proliferative potential of stem cells. In particular, *TgTert* mice have longer telomeres in different epithelia at both young and old ages. As telomere length influences the ability of epidermal stem cells to mobilize and to regenerate tissues (Flores et al., 2005), it is conceivable that longer telomeres in young individuals may result in an increased regenerative capacity of tissues. In particular, a better preservation of telomeres at young ages may affect the proliferative potential and regenerative capacity of tissues, in agreement with the fact that young *TgTert* mice present a better fitness in a number of assays, such as improved GI tract barrier function, increased clonogenic activity, and improved glucose tolerance. Also in agreement with this notion, we have previously shown that *TgTert* mice have augmented proliferative responses already at very young ages (González-Suárez et al., 2001; Flores et al., 2005) and that these proliferative phenotypes require an active telomerase complex (i.e., the *Terc* RNA component) (Cayuela et al., 2005; Flores et al., 2005). These observations suggest that telomere loss, even at young ages, may limit the proliferation of a fraction of cells, including the stem cells and, therefore, telomere maintenance is relevant not only for aging but also for the optimal fitness of young organisms. Importantly, we demonstrate here that the longevity effects of *TgTert* expression require its telomere-maintenance activity, as *TgTert* expression did not modify the longevity curve of *Terc*-deficient mice across four mouse generations. These observations strongly implicate telomere-maintenance as the main mechanism underlying the antiaging activity of TERT. There are, however, nontelomeric activities of TERT (Sarin et al., 2005; Choi et al., 2008), which could also conceivably contribute to the antiaging phenotypes reported here. Finally, it is worth highlighting that we have observed an improved fitness in organs that do not express *TgTert*, such as the brain or muscle (i.e., neuromuscular coordination assay), suggesting that *TgTert* expression has systemic antiaging effects. It will be of great interest to study the impact of ubiquitous *TgTert* expression on mouse fitness and longevity.

Figure 5. Increased Longevity of *Sp53/Sp16/SArf/TgTert* Mice

(A) Survival curves (Kaplan-Meier representation) of the indicated mouse cohorts. Only mice that reached at least up to 50 weeks of age were included. n = number of mice per genotype. Mice alive at the time of the quantification are indicated in the curves with small bars. Statistical significance was assessed using the log rank test.

(B) Percentage of mice living for more than three years (bar graph) of the indicated mouse cohorts. Only mice that reached their maximum life span are included (n). Statistical significance was assessed using the χ^2 test.

(C) Average life span of mice belonging to the upper longevity quartile in the indicated genotypes. Each dot represents an individual mouse. Statistical significance comparisons are indicated.

(D) Survival curves (Kaplan-Meier representation) of the indicated mouse cohorts. Only mice that reached their maximum life span are included (n).

(E) Percentage of mice of the indicated genotypes showing the indicated malignant tumors at the time of death. Only mice that reached their maximum life span are included (n). Percentage of mice showing degenerative lesions of the skin (F) or in the GI tract (G), which are associated with loss of epithelial barrier. Statistical comparisons using the χ^2 test are shown. Only mice that reached their maximum life span are included (n).

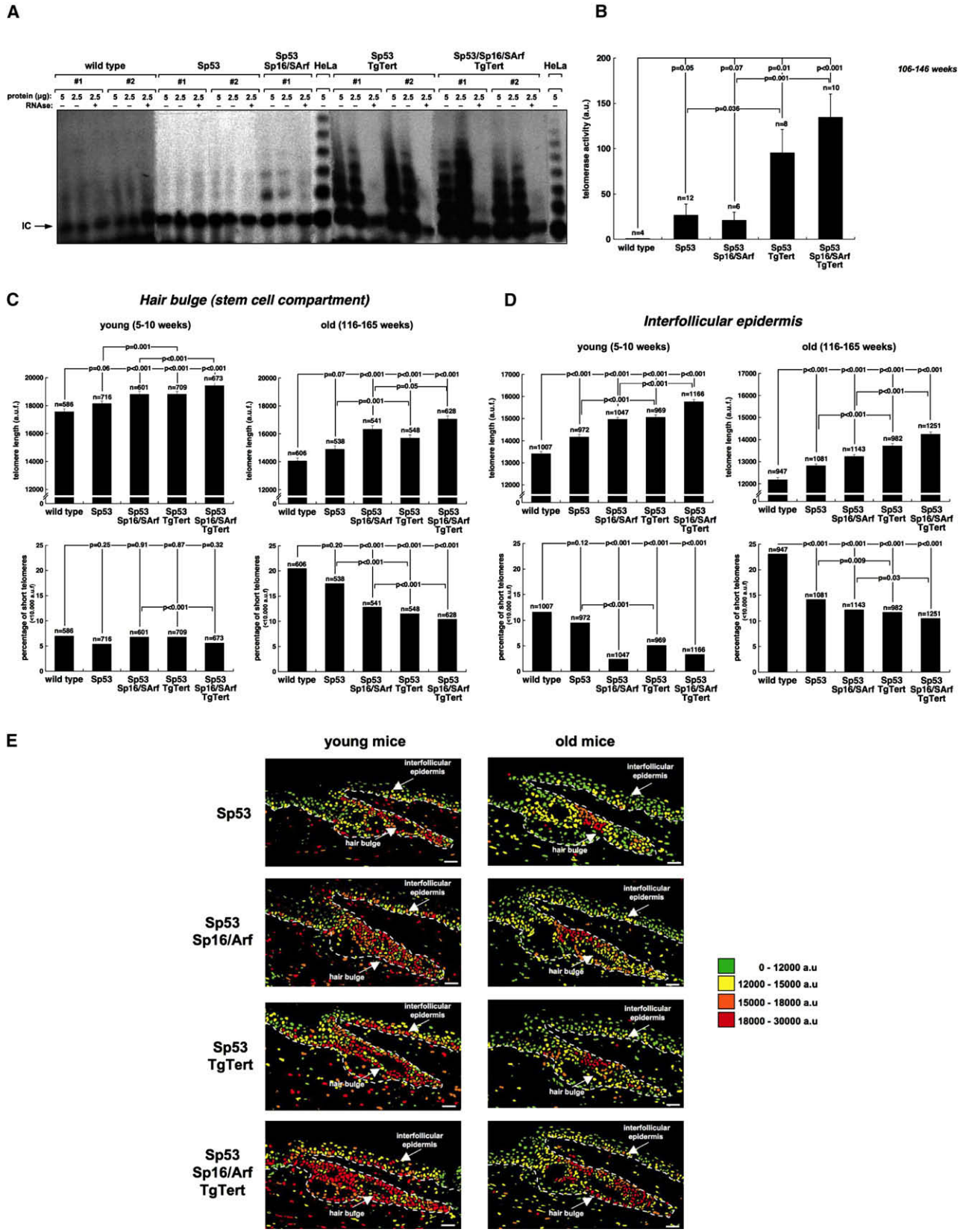
A
wild type
Sp53
Sp53 Sp16/SArf
HeLa
Sp53 TgTert
Sp53/Sp16/SArf TgTert
HeLa
protein (µg):
RNAse:
IC
B
telomerase activity (a.u.)
106-146 weeks
wild type
Sp53
Sp53 Sp16/SArf
Sp53 TgTert
Sp53 Sp16/SArf TgTert
C
Hair bulge (stem cell compartment)
young (5-10 weeks)
old (116-165 weeks)
telomere length (a.u.f.)
percentage of short telomeres
D
Interfollicular epidermis
young (5-10 weeks)
old (116-165 weeks)
E
young mice
old mice
Sp53
Sp53 Sp16/Arf
Sp53 TgTert
Sp53 Sp16/Arf TgTert
interfollicular epidermis
hair bulge
0 - 12000 a.u
12000 - 15000 a.u
15000 - 18000 a.u
18000 - 30000 a.u

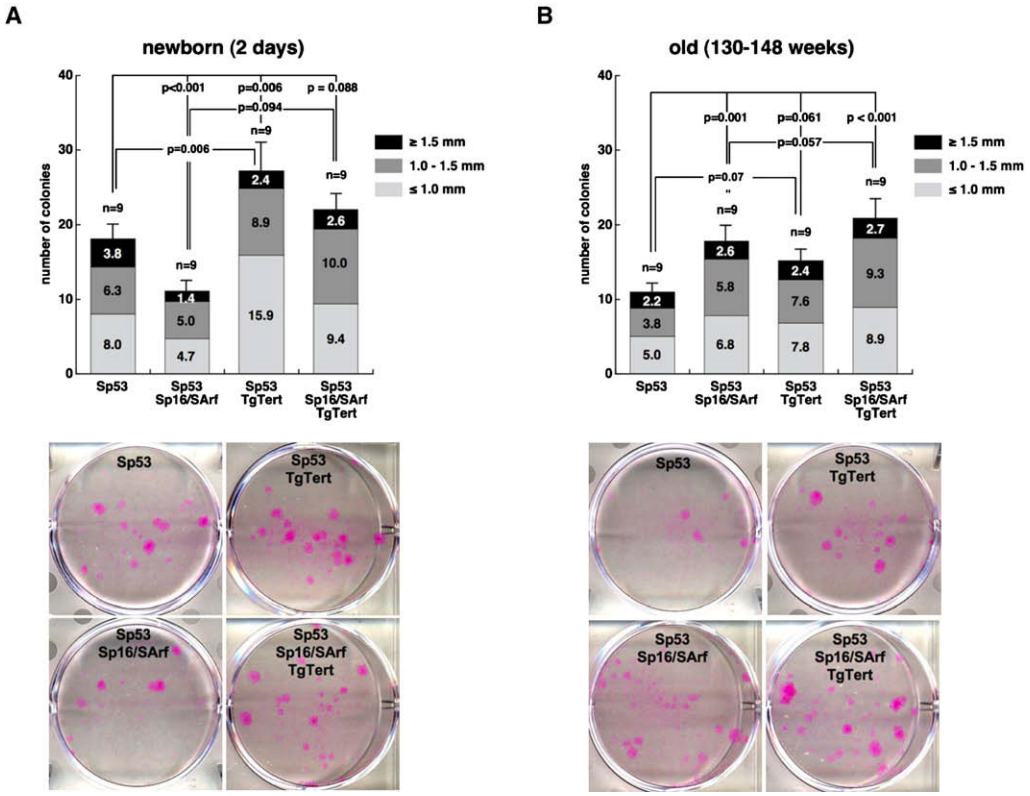

Figure 7. Increased ESC Clonogenic Activity in *Sp53/Sp16/SArf/TgTert* Mice

Number and size of colonies obtained from newborn (A) and aged (B) keratinocytes. Data are given as mean ± SEM, and statistical comparisons were made using the Student's t test. n, number of keratinocyte cultures from a total of three mice of each genotype. Representative images of colonies are shown below each graph.

Interestingly, we have observed that the rate of telomere loss with aging is also slowed by the p53 and by the p16/p19ARF tumor suppressor transgenes. These tumor suppressors have been involved in restraining the proliferation of adult stem cells (Meletis et al., 2006; Molofsky et al., 2006; Janzen et al., 2006; Krishnamurthy et al., 2006). Therefore, the lower rate of telomere attrition in *Sp53/Sp16/SArf* mice is in agreement with a slower rate of stem cell division in these transgenic mice. A slower rate of stem cell proliferation can be beneficial because it may help to preserve stem cell quiescence and maintain stem cell pools at old ages, as reported for the p53 target p21 (Cheng et al., 2000; Kippin et al., 2005). Similarly, moderately increased cell-cycle inhibitors provided by the p19ARF/p53 pathway in our *Sp53/Sp16/SArf* transgenic mice may result in a reduced pace of stem cell division throughout the life of mice and in better preserved telomeres at stem cell niches at old ages. In addition, augmented activity of the p19ARF/p53 pathway in *Sp53/Sp16/SArf* transgenic mice results in decreased DNA damage with age, probably because of better elimination of damaged cells by senescence and/or apoptosis (Matheu et al., 2007). A simultaneous increase in telomerase activity would further postpone the exhaustion/malfunction of stem cells by maintaining their telomeres during longer times and delaying telomere-associated DNA damage, thus resulting in fewer degenerative lesions and overall life span extension. Therefore, we propose that *Tert* and *Sp53/Sp16/SArf* expression synergize in preserving telomere length in stem cells—in the case of *Tert* expression through direct extension of telomeres, and in the case of *Sp53/Sp16/SArf* by slowing the rate of proliferation. Finally, it is worth mentioning that the combined effects of *TgTert*

Figure 6. Decreased Aging-Associated Telomere Loss in *Sp53/Sp16/SArf/TgTert* Mice

(A) Telomerase activity in keratinocytes. Extracts were treated (+) or not (−) with RNase as a negative control. An internal control (IC) for PCR efficiency was also included. HeLa cells were used as positive control. Data are given as mean ± SEM; statistical comparisons were made using the Student's t test.

(B) n, number of independent experiments using 2–4 mice per genotype.

(C–E) Telomapping shows longer telomeres in both the stem cell (hair bulge) and differentiated (interfollicular epidermis) skin compartments of *Sp53/Sp16/SArf/TgTert* mice. Data are given as mean ± SEM; n, total number of telomere signals out of at least 4 mice per genotype and age group. For full-telomere length histograms, see Figure S11. Statistical comparisons were made using the Wilcoxon-Mann-Whitney rank sum test (telomere length) and the χ^2 test (percentage of short telomeres). Representative telomere length pseudo-color images from skin sections (E). Nuclei are colored according to their average telomere fluorescence in arbitrary units (a.u.). Note an enrichment of cells with the longest telomeres at the hair bulge area in the case of old *Sp53*/Sp16S/SArf/*TgTert* mice. Scale bars correspond to 50 μM.

and *Sp53/Sp16/SArf* transgenes on median mouse longevity are of similar magnitude to those produced by calorie restriction, by decreased growth hormone (GH)/IGF1 signaling, or by abrogation of the type 5 adenylyl cyclase (Weindruch et al., 1986; Brown-Borg et al., 1996; Yan et al., 2007).

Together, these observations demonstrate the antiaging effects of telomerase in the context of living organisms and provide further support to the important contribution of telomere biology to aging.

EXPERIMENTAL PROCEDURES

Mice

Mice were housed at the pathogen-free barrier area of the CNIO, in accordance with the recommendations of the Federation of European Laboratory Animal Science Associations. Mice were observed daily and sacrificed when they showed signs of morbidity or tumors in accordance to the Guidelines for Humane Endpoints for Animals Used in Biomedical Research. *Sp53*, *Sp53/Sp16/SArf*, *Sp53/TgTert*, and *Sp53/Sp16/SArf/TgTert* mice, as well as their wild-type controls, have a 75% C57BL6, 25% DBA/2 genetic background and were derived from the same parents by crossing *K5-Tert* females (C57BL6-DBA/2 background) (González-Suárez et al., 2001) with *Sp53/Sp16/SArf* males (100% C57BL6 background) (Matheu et al., 2007). In parallel, *Sp53* and *Sp53/Sp16/SArf* mice were maintained in the original 100% C57BL6 background (Figure S8).

Mice shown in Figures 5D–5G have a 100% C57Bl6 genetic background (Cayuela et al., 2005). Mice within each $Terc^{-/-}$ mouse generation are littermates.

Skin and Small Intestine Epithelia Measurements

Epidermal and subcutaneous fat layer thickness and intestinal villi length were determined using 10–74 random measurements along the length of skin and small intestine from at least 3 mice per age group and genotype. For skin sections, the skin was cut parallel to the spine and sections were cut perpendicular to the skin surface. For villi sections, intestinal tracts were flushed with PBS and rolled up in a compact circle using longitudinally oriented jejunal sections for analysis; 5 μM sections were used for hematoxylin-eosin staining, and Image J software was used for length measurements.

Induction of Intestinal Ulcers

Ulcers were induced as described elsewhere (Rakoff-Nahoum et al., 2004). Briefly, 5 mice per genotype received 2% (wt/vol) DSS (36,000 kDa; MP Biomedicals) in their drinking water for 7 days. Feces (21 fecal pellets per genotype) were analyzed at days 3, 5, and 7 for the presence of blood using the ColoScreen test (Helena Laboratories). At day 7, large intestines were excised, fixed in formalin, and embedded in paraffin. Hematoxylin-eosin slides, separating 200 μm and spanning the whole paraffin block, were analyzed to score the number, size, and grade of ulcers. Histological scoring was made as follows: Grade 0, normal colon; Grade 1, mild inflammation in lamina propria with mixed component (neutrophils and plasma cells), hyperplasia of goblet cells, and disorganized crypts, with frequent fusions between them; Grade 2, moderate inflammation in lamina propria and signs of regenerative dysplasia (frequent mitosis, loss of crypt polarization, and decreased number of goblet cells); Grade 3, severe inflammation in lamina propria, with a high proportion of neutrophils, single-cell layer of epithelium without crypts, and frequent edema; and Grade 4, severe inflammation in lamina propria, with high proportion of neutrophils, lamina propria directly exposed to the light of the colon, with no epithelium lining it, and frequent edema. Final histological score was calculated as the sum of the factors obtained by multiplying size and histological score for every ulcer.

Tightrope Test (Neuromuscular Coordination Assay)

The tightrope test was performed as described elsewhere (Ingram and Reynolds, 1986; Matheu et al., 2007). Briefly, mice were placed on a bar of circular section (60 cm long and 1.5 cm diameter) and the test was considered successful when a mouse did not fall during a period of 60 s in at least one trial out of 5 consecutive trials.

Intraperitoneal Glucose Tolerance Tests

Glucose curves were performed as described elsewhere (Moynihan et al., 2005). Briefly, males were fasted for 15 hr, and then i.p.-injected with 50% dextrose (2 g/kg body weight). Tail blood glucose levels were measured with a glucometer (Glucocard Memory 2, Arkray, Japan) at the indicated times after injection. Standard glucose curves were represented, and area under the curve (AUC) was calculated.

Measurements of IGF1 Levels

Renal or retro-orbital cavity blood was extracted, and after 5 min at room temperature, samples were centrifuged at 1,600 × g for 5 min at 4°C. Supernatants (serum) were collected and stored at −80°C. Serum levels of IGF1 were measured using commercial kits (Rat/Mouse IGF1 EIA DSL-10-2900 from Diagnostic Systems Laboratorie or Rat/Mouse IGF1 ELISA from GroPep).

Quantification of Phosphorylated H2AX Foci and of Telomere-Induced Foci

Phosphorylated H2AX foci were detected using a mouse monoclonal anti-phospho-histone H2AX antibody (1:500; from Upstate Biotechnology) as described elsewhere (Muñoz et al., 2005). Sections from γ-irradiated mice were used as positive controls. Mice were irradiated with a dose of 10 Gy using a ^{137}Cs source (MARK 1-30 irradiator; Shepherd & Associates) at a rate of 2.11 Gy/min. Images were obtained with a confocal ultra-spectral microscope (Leica TCS-SP2-A-OBS-UV) and a Leica CTR MIC microscope equipped with a COHU High-Performance CCD camera. A cell was positive for γ-H2AX staining when it showed two or more foci.

For TRF1-γ-H2AX colocalization (TIF), after incubation with the γ-H2AX antibody described above, a second staining was performed with rabbit anti-mTRF1 (1:100) (Muñoz et al., 2005) overnight at 4°C. Then tissues were rinsed 3 times with PBS and incubated with goat anti-rabbit Alexa 488 (1:400) (Molecular Probes). Skin sections were mounted with Vectashield with 4′,6-diamino-2 phenylindole (DAPI). Images were obtained as described above. A positive colocalization was considered when one or more TRF1 foci could be superimposed to γ-H2AX foci.

Isolation of Keratinocytes

Keratinocytes from newborn mice were isolated as described previously (Flores et al., 2005). Adult skin keratinocyes were isolated as described elsewhere (Muñoz et al., 2005).

Telomeric Repeat Amplification Protocol

Telomeric repeat amplification (TRAP) reactions of freshly isolated adult keratinocytes were performed as described elsewhere (Blasco et al., 1997). As negative control, extracts were preincubated with 5 μg RNase for 10 min at 30°C before the extension reaction. As a positive control, telomerase-positive HeLa cells were included. An internal control for PCR efficiency was included (IC) (TRAPeze kit Oncor, Gaithersburg, MD).

Generation of Telomere Length Maps on Histological Sections or "Telomapping"

Quantitative image analysis was performed on confocal images using the Metamorph platform (version 6.3r6; Molecular Devices, Union City, CA) as described elsewhere (Flores et al., 2008).

Colony Forming Assay

One thousand mouse keratinocytes obtained from newborn mice and ten thousand mouse keratinocytes obtained from old mice were used in clonogenic assays as described elsewhere (Flores et al., 2005).

Statistical Analyses

To calculate statistical significance of pathological analyses (malignant tumors, lesions associated with the loss of epithelial barrier, and degenerative lesions of the skin and the GI tract) as well as for calculation of the time of onset of malignant tumors and the age-related pathologies the χ^2 test was used. The

two-sided p values were obtained from a 2 × 2 contingency table analyzed by the χ^2 test (including Yate's continuity correction). A t-student test with two tails, two samples of unequal variance (or Welch's correction), was used to calculate statistical significance of thickness of the epidermal and subcutaneous fat layers, histological score of ulcers, glucose tolerance, IGF-1 ELISA analysis, TRAP, colony forming assay, food and water intake controls, and the measurement of the oxidative damage. The Fisher's exact test was used to calculate statistical differences in γ-H2AX foci and TIFs, as well as for calculation of survival at three years, analysis of blood in feces, and the neuromuscular coordination assay. The Wilcoxon-Mann-Whitney rank sum test was used to calculate the statistical significance of the observed differences in telomere length. Finally, a log rank test was used to calculate the statistical differences in the survival of the different mouse cohorts. Microsoft Excel version 2003 and GraphPad Instat version 2.03 were used for calculations.

SUPPLEMENTAL DATA

Supplemental Data include Supplemental Experimental Procedures, Supplemental References, and 12 figures and can be found with this article online at http://www.cell.com/supplemental/S0092-8674(08)01191-4.

ACKNOWLEDGMENTS

A.T. is a predoctoral fellow of the Regional Government of Madrid. I.F. is a Ramon y Cajal scientist. M.A.B.'s laboratory is funded by the Ministry of Science and Innovation of Spain, by the European Union, by the Körber European Science Award, and by the Spanish Association Against Cancer. M.S.'s laboratory is funded by the Ministry of Science and Innovation of Spain, by the European Union, and by the Fundacíon Marcelino Botin.

Received: February 15, 2008
Revised: June 18, 2008
Accepted: September 15, 2008
Published: November 13, 2008

REFERENCES

Armanios, M.Y., Chen, J.J., Cogan, J.D., Alder, J.K., Ingersoll, R.G., Markin, C., Lawson, W.E., Xie, M., Vulto, I., Phillips, J.A., 3rd, Lansdorp, P.M., Greider, C.W., and Loyd, J.E. (2007). Telomerase mutations in families with idiopathic pulmonary fibrosis. N. Engl. J. Med. *356*, 1317–1326.

Artandi, S.E., Alson, S., Tietze, M.K., Sharpless, N.E., Ye, S., Greenberg, R.A., Castrillon, D.H., Horner, J.W., Weiler, S.R., Carrasco, R.D., and DePinho, R.A. (2002). Constitutive telomerase expression promotes mammary carcinomas in aging mice. Proc. Natl. Acad. Sci. USA *99*, 8191–8196.

Barrandon, Y., and Green, H. (1987). Three clonal types of keratinocyte with different capacities for multiplication. Proc. Natl. Acad. Sci. USA *84*, 2302–2306.

Blackburn, E.H. (2001). Switching and signaling at the telomere. Cell *106*, 661–673.

Blasco, M.A., Lee, H.W., Hande, M.P., Samper, E., Lansdorp, P.M., DePinho, R.A., and Greider, C.W. (1997). Telomere shortening and tumor formation by mouse cells lacking telomerase RNA. Cell *91*, 25–34.

Blasco, M.A. (2005). Telomeres and human disease: ageing, cancer and beyond. Nat. Rev. Genet. Nat. Rev. Genet. *6*, 611–622.

Blasco, M.A. (2007). Telomere length, stem cells and aging. Nat. Chem. Biol. *3*, 640–649.

Bodnar, A.G., Ouellette, M., Frolkis, M., Holt, S.E., Chiu, C.P., Morin, G.B., Harley, C.B., Shay, J.W., Lichtsteiner, S., and Wright, W.E. (1998). Extension of life-span by introduction of telomerase into normal human cells. Science *279*, 349–352.

Brown-Borg, H.M., Borg, K.E., Meliska, C.J., and Bartke, A. (1996). Dwarf mice and the ageing process. Nature *384*, 33.

Blüher, M., Kahn, B.B., and Kahn, C.R. (2003). Extended longevity in mice lacking the insulin receptor in adipose tissue. Science *299*, 572–574.

Buchkovich, K.J., and Greider, C.W. (1996). Telomerase regulation during entry into the cell cycle in normal human T cells. Mol. Biol. Cell *7*, 1443–1454.

Canela, A., Martin-Caballero, J., Flores, J.M., and Blasco, M.A. (2004). Constitutive expression of tert in thymocytes leads to increased incidence and dissemination of T-cell lymphoma in Lck-Tert mice. Mol. Cell. Biol. *24*, 4275–4293.

Cayuela, M.L., Flores, J.M., and Blasco, M.A. (2005). The telomerase RNA component, Terc, is required for the telomere-length independent tumor promoting effects of Tert over-expression. EMBO Rep. *6*, 268–274.

Cheng, T., Rodrigues, N., Shen, H., Yang, Y., Dombkowski, D., Sykes, M., and Scadden, D.T. (2000). Hematopoietic stem cell quiescence maintained by p21cip1/waf1. Science *287*, 1804–1808.

Choi, J., Southworth, L.K., Sarin, K.Y., Venteicher, A.S., Ma, W., Chang, W., Cheung, P., Jun, S., Artandi, M.K., Shah, N., Kim, S.K., and Artandi, S.E. (2008). TERT promotes epithelial proliferation through transcriptional control of a Myc- and Wnt-related developmental program. PLoS Genet. *4*, e10.

Collado, M., Blasco, M.A., and Serrano, M. (2007). Cellular senescence in cancer and aging. Cell *130*, 223–233.

Conboy, I.M., Conboy, M.J., Wagers, A.J., Girma, E.R., Weissman, I.L., and Rando, T.A. (2005). Rejuvenation of aged progenitor cells by exposure to a young systemic environment. Nature *433*, 760–764.

d'Adda di Fagagna, F., Reaper, P.M., Clay-Farrace, L., Fiegler, H., Carr, P., Von Zglinicki, T., Saretzki, G., Carter, N.P., and Jackson, S.P. (2003). A DNA damage checkpoint response in telomere-initiated senescence. Nature *426*, 194–198.

de Lange, T. (2005). Shelterin: the protein complex that shapes and safeguards human telomeres. Genes Dev. *19*, 2100–2110.

Delbono, O. (2003). Neural control of aging skeletal muscle. Aging Cell *2*, 21–29.

Feldser, D.M., and Greider, C.W. (2007). Short telomeres limit tumor progression in vivo by inducing senescence. Cancer Cell *11*, 461–469.

Flores, I., Cayuela, M.L., and Blasco, M.A. (2005). Effects of telomerase and telomere length on epidermal stem cell behavior. Science *309*, 1253–1256.

Flores, I., Evan, G., and Blasco, M.A. (2006). Genetic analysis of Myc and telomerase interactions *in vivo*. Mol. Cell. Biol. *26*, 6130–6138.

Flores, I., Canela, A., Vera, E., Tejera, A., Cotsarelis, G., and Blasco, M.A. (2008). The longest telomeres: a general signature of adult stem cell compartments. Genes Dev. *22*, 654–667.

Garcia-Cao, I., Garcia-Cao, M., Martin-Caballero, J., Criado, L.M., Klatt, P., Flores, J.M., Weill, J.C., Blasco, M.A., and Serrano, M. (2002). "Super p53" mice exhibit enhanced DNA damage response, are tumor resistant and age normally. EMBO J. *21*, 6225–6235.

Garcia-Cao, I., Garcia-Cao, M., Tomas-Loba, A., Martin-Caballero, J., Flores, J.M., Klatt, P., Blasco, M.A., and Serrano, M. (2006). Increased p53 activity does not accelerate telomere-driven ageing. EMBO Rep. *7*, 546–552.

González-Suárez, E., Samper, E., Ramirez, A., Flores, J.M., Martin-Caballero, J., Jorcano, J.L., and Blasco, M.A. (2001). Increased epidermal tumors and increased skin wound healing in transgenic mice overexpressing the catalytic subunit of telomerase, mTERT, in basal keratinocytes. EMBO J. *20*, 2619–2630.

González-Suárez, E., Flores, J.M., and Blasco, M.A. (2002). Cooperation between p53 mutation and high telomerase transgenic expression in spontaneous cancer development. Mol. Cell. Biol. *22*, 7291–7301.

Goren, H.J., Kulkarni, R.N., and Kahn, C.R. (2004). Glucose homeostasis and tissue transcript content of insulin signaling intermediates in four inbred strains of mice: C57BL/6, C57BLKS/6, DBA/2, and 129X1. Endocrinology *145*, 3307–3323.

Greider, C.W., and Blackburn, E.H. (1985). Identification of a specific telomere terminal transferase activity in Tetrahymena extracts. Cell *43*, 405–413.

Haigis, M.C., and Guarente, L.P. (2006). Mammalian sirtuins—emerging roles in physiology, aging, and calorie restriction. Genes Dev. *20*, 2913–2921.

Hammerman, M.R. (1987). Insulin-like growth factors and aging. Endocrinol. Metab. Clin. North Am. *16*, 995–1011.

Harley, C.B., Futcher, A.B., and Greider, C.W. (1990). Telomeres shorten during ageing of human fibroblasts. Nature *345*, 458–460.

Herbig, U., Ferreira, M., Condel, L., Carey, D., and Sedivy, J.M. (2006). Cellular senescence in aging primates. Science *311*, 1257.

Ingram, D.K., and Reynolds, M.A. (1986). Assessing the predictive validity of psychomotor tests as measures of biological age in mice. Exp. Aging Res. *12*, 155–162.

Janzen, V., Forkert, R., Fleming, H.E., Saito, Y., Waring, M.T., Dombkowski, D.M., Cheng, T., DePinho, R.A., Sharpless, N.E., and Scadden, D.T. (2006). Stem-cell ageing modified by the cyclin-dependent kinase inhibitor p16INK4a. Nature *443*, 421–426.

Kenyon, C. (2005). The plasticity of aging: insights from long-lived mutants. Cell *120*, 449–460.

Kippin, T.E., Martens, D.J., and van der Kooy, D. (2005). p21 loss compromises the relative quiescence of forebrain stem cell proliferation leading to exhaustion of their proliferation capacity. Genes Dev. *19*, 756–767.

Krishnamurthy, J., Torrice, C., Ramsey, M.R., Kovalev, G.I., Al-Regaiey, K., Su, L., and Sharpless, N.E. (2004). Ink4a/Arf expression is a biomarker of aging. J. Clin. Invest. *114*, 1299–1307.

Krishnamurthy, J., Ramsey, M.R., Ligon, K.L., Torrice, C., Koh, A., Bonner-Weir, S., and Sharpless, N.E. (2006). p16INK4a induces an age-dependent decline in islet regenerative potential. Nature *443*, 453–457.

Matheu, A., Pantoja, C., Efeyan, A., Criado, L.M., Martin-Caballero, J., Flores, J.M., Klatt, P., and Serrano, M. (2004). Increased gene dosage of Ink4a/Arf results in cancer resistance and normal aging. Genes Dev. *18*, 2736–2746.

Matheu, A., Maraver, A., Klatt, P., Flores, I., Garcia-Cao, I., Borras, C., Flores, J.M., Viña, J., Blasco, M.A., and Serrano, M. (2007). Delayed aging through damage protection by the Arf/p53 pathway. Nature *448*, 375–379.

Meletis, K., Wirta, V., Hede, S.M., Nistér, M., Lundeberg, J., and Frisén, J. (2006). p53 suppresses the self-renewal of adult neural stem cells. Development *133*, 363–369.

Mitchell, J.R., Wood, E., and Collins, K. (1999). A telomerase component is defective in the human disease dyskeratosis congenita. Nature *402*, 551–555.

Molofsky, A.V., Slutsky, S.G., Joseph, N.M., He, S., Pardal, R., Krishnamurthy, J., Sharpless, N.E., and Morrison, S.J. (2006). Increasing p16INK4a expression decreases forebrain progenitors and neurogenesis during ageing. Nature *443*, 448–452.

Moynihan, K.A., Grimm, A.A., Plueger, M.M., Bernal-Mizrachi, E., Ford, E., Cras-Méneur, C., Permutt, M.A., and Imai, S. (2005). Increased dosage of mammalian Sir2 in pancreatic beta cells enhances glucose-stimulated insulin secretion in mice. Cell Metab. *2*, 105–117.

Murphy, C.T., McCarroll, S.A., Bargmann, C.I., Fraser, A., Kamath, R.S., Ahringer, J., Li, H., and Kenyon, C. (2003). Genes that act downstream of DAF-16 to influence the lifespan of *Caenorhabditis elegans*. Nature *424*, 277–283.

Muñoz, P., Blanco, R., Flores, J.M., and Blasco, M.A. (2005). XPF nuclease-dependent telomere loss and increased DNA damage in mice overexpressing TRF2 result in premature aging and cancer. Nat. Genet. *10*, 1063–1071.

Niedernhofer, L.J., Garinis, G.A., Raams, A., Lalai, A.S., Robinson, A.R., Appeldoorn, E., Odijk, H., Oostendorp, R., Ahmad, A., van Leeuwen, W., et al. (2006). A new progeroid syndrome reveals that genotoxic stress suppresses the somatotroph axis. Nature *444*, 1038–1043.

Rakoff-Nahoum, S., Paglino, J., Eslami-Varzaneh, F., Edberg, S., and Medzhitov, R. (2004). Recognition of commensal microflora by toll-like receptors is required for intestinal homeostasis. Cell *118*, 229–241.

Ramírez, A., Bravo, A., Jorcano, J.L., and Vidal, M. (1994). Sequences 5′ of the bovine keratin 5 gene direct tissue- and cell-type-specific expression of a lacZ gene in the adult and during development. Differentiation *58*, 53–64.

Sablina, A.A., Budanov, A.V., Ilyinskaya, G.V., Agapova, L.S., Kravchenko, J.E., and Chumakov, P.M. (2005). The antioxidant function of the p53 tumor suppressor. Nat. Med. *11*, 1306–1313.

Sarin, K.Y., Cheung, P., Gilison, D., Lee, E., Tennen, R.I., Wang, E., Artandi, M.K., Oro, A.E., and Artandi, S.E. (2005). Conditional telomerase induction causes proliferation of hair follicle stem cells. Nature *436*, 1048–1052.

Sedelnikova, O.A., Horikawa, I., Zimonjic, D.B., Popescu, N.C., Bonner, W.M., and Barrett, J.C. (2004). Senescing human cells and ageing mice accumulate DNA lesions with unrepairable double-strand breaks. Nat. Cell Biol. *6*, 168–170.

Tsakiri, K.D., Cronkhite, J.T., Kuan, P.J., Xing, C., Raghu, G., Weissler, J.C., Rosenblatt, R.L., Shay, J.W., and Garcia, C.K. (2007). Adult-onset pulmonary fibrosis caused by mutations in telomerase. Proc. Natl. Acad. Sci. USA *104*, 7552–7557.

Vulliamy, T., Marrone, A., Goldman, F., Dearlove, A., Bessler, M., Mason, P.J., and Dokal, I. (2001). The RNA component of telomerase is mutated in autosomal dominant dyskeratosis congenita. Nature *413*, 432–435.

Weindruch, R., Walford, R.L., Fligiel, S., and Guthrie, D. (1986). The retardation of aging in mice by dietary restriction: longevity, cancer, immunity and lifetime energy intake. J. Nutr. *116*, 641–654.

Yan, L., Vatner, D.E., O'Connor, J.P., Ivessa, A., Ge, H., Chen, W., Hirotani, S., Ishikawa, Y., Sadoshima, J., and Vatner, S.F. (2007). Type 5 adenylyl cyclase disruption increases longevity and protects against stress. Cell *130*, 247–258.

Yamaguchi, H., Calado, R.T., Ly, H., Kajigaya, S., Baerlocher, G.M., Chanock, S.J., Lansdorp, P.M., and Young, N.S. (2005). Mutations in TERT, the gene for telomerase reverse transcriptase, in aplastic anemia. N. Engl. J. Med. *352*, 1413–1424.

Yuen, K.C., and Dunger, D.B. (2007). Therapeutic aspects of growth hormone and insulin-like growth factor-I treatment on visceral fat and insulin sensitivity in adults. Diabetes Obes. Metab. *9*, 11–22.

Zindy, F., Quelle, D.E., Roussel, M.F., and Sherr, C.J. (1997). Expression of the p16INK4a tumor suppressor versus other INK4 family members during mouse development and aging. Oncogene *15*, 203–211.